ARPN Journal of Engineering and Applied Sciences


www.arpnjournals.com

# VORTEX IN CELL METHOD TO PREDICT FLUTTER PHENOMENON OF 2D BRIDGE DECK MODEL

Eky V. Febrianto and Lavi R. Zuhal
Faculty of Mechanical and Aerospace Engineering, Bandung Institute of Technology Jalan Ganesa, Bandung, Indonesia
E-Mail: lavirz@ae.itb.ac.id

**ABSTRACT**

The Vortex-In-Cell (VIC) comes as an alternative of the two major CFD methods, the mesh-based and mesh-free method. As a hybrid method, VIC uses particles as discrete model of the fluid domain (mesh-free method) and also employs rectangular grid system to evaluate the governing equation (mesh-based method). The use of grid allows the use of finite difference stencils to discretize the equation. An immersed boundary model called Brinkman Penalization is utilized as solid boundary condition. The method creates solid mask in fluid domain by the implementation of a mollified step function to distinguish the solid from the fluid region. Therefore, it is possible to simulate flow around multiple complex, moving, and deforming geometries. The performance of the code to simulate moving body is tested by simulating fluid-structure interaction (FSI) and flutter phenomena of long-span bridges. The result of the simulations shows good agreement with another numerical method and experimental work.

**Keywords:** vortex in cell, computational fluid dynamics, flutter speed, flutter derivatives.

## INTRODUCTION

CFD had been used in a very wide-range applications of fluid dynamics, including bridge aerodynamics. Analysis of fluid interaction with bridge structure needs to be performed as a part of safety design since the Tacoma Narrows Bridge catastrophe in 1949. The two major kinds of CFD, the mesh-based (Eulerian) and mesh-free/particle (Lagrangian), had been applied to do this analysis. To simulate moving body with Eulerian method, the grid should be generated and refined every time step, which contributes to the high computational cost. The Lagrangian CFD can overcome this challenge, but its cost will also escalate due to the need to compute Biot-Savart integration scheme. The Vortex in Cell is a hybrid method which uses particles and also rectangular grid system to perform computation of fluid properties. The grid is also used to define the solid boundary by introducing an immersed boundary method called Brinkman penalization. The penalization allows us to simulate flow around any complex, moving, and deforming bodies conveniently. The VIC is then employed to acquire aerodynamic loads to calculate flutter derivatives. The derivatives are then used to predict critical speed before the occurrence of flutter. To investigate the performance of the method, flutter instability analysis of a long span bridge with two degree of freedom (heaving and pitching) is performed.

## NUMERICAL MODEL

### The vortex in cell (VIC) method general algorithm

Given the general equation of a moving fluid particle inside an incompressible flow as the following:

$$\frac{\partial \underline{u}}{\partial t} + (\underline{u}.\nabla)\underline{u} = -\frac{1}{\rho}\nabla p + \nu\nabla^2 \underline{u}. \qquad \nabla.\underline{u} = 0 \tag{1}$$

with constant kinematic viscosity $\upsilon$. Both are well known as Navier-Stokes equation which entails the conservation of momentum and conservation of mass. The conservation of momentum equation sums the contributions from its components: the unsteady, convective, pressure gradient and viscous terms. Taking curl of Navier-Stokes equation, the vorticity-velocity formulation thus reads:

$$\frac{\partial \underline{\omega}}{\partial t} + (\underline{u}.\nabla)\underline{\omega} = (\underline{\omega}.\nabla)\underline{u} + \nu\nabla^2 \underline{\omega}, \tag{2}$$

The vorticity evolution depends on three distinct terms: the convection, the stretching and the diffusion. For two-dimensional flows, the stretching term drops out. We may reform both terms in the left hand side into one total derivative of vorticity thus confirms the vorticity transport equation:

$$\frac{d\omega}{dt} = \nu\nabla^2 \omega. \tag{3}$$

The reformed Navier-Stokes (equation 3) can be divided into two sub-steps following Chorin's algorithm as the following [12]:

A. Sub-step 1: Convection

$$\frac{d\omega}{dt} = \frac{\partial \omega}{\partial t} + \underline{u}\cdot\nabla\omega \left\langle \begin{array}{l} \dfrac{d\underline{X}}{dt} = u \\ \dfrac{d\omega}{dt} = 0 \end{array} \right. \tag{4}$$

B. Sub-step 2: Diffusion

$$\frac{\partial \omega}{dt} = \nu\nabla^2 \omega \tag{5}$$

ARPN Journal of Engineering and Applied Sciences



On the first sub-step, we consider that particle is moving on the domain using Lagrangian convection scheme. Particle's position will be updated following the time integration scheme with velocity $\underline{u}$, while its vorticity remains constant during the motion. The second sub-step works on evaluating vorticity on the grid by calculating diffusion term. The relation between grid and particles is provided by interpolation scheme both from particle to mesh (P2M remeshing) and mesh to particle (M2P remeshing).

**Poisson's solver**

The vorticity in two-dimensional analysis is defined as scalar produced by the curl of the velocity field [10]. As velocity disappears from the governing equation (equation 3), a relation between vorticity and velocity needs to be stated. The VIC will make use of stream function as a link of two quantities as shown in the following expression:

$$u = \nabla \times \psi . + U_{\infty} \quad (6)$$

where $\psi$ is the associated stream function and $U_{\infty}$ is irrotational stream velocity. Combining equation 6 with vorticity definition we get the Poisson equation

$$\nabla^2 \psi . = -\omega \quad (7)$$

To solve Poisson's equation we introduce rectangular grid system on which the vorticity of the particles is interpolated, thus equation 6 and 7 can be easily solved by applying finite difference stencils. We use point iterative successive over relaxation (PSOR) method as Poisson's equation solver. The PSOR is built on the motivation to improve Jacobi method and Gauss-Seidel algorithm by introducing an over-relaxation parameter ($\mu$) to speed up the convergence.

**Remeshing scheme**

One of the main problems of Lagrangian method maybe particles' irregularity after some time steps as particles adapt to the gradient of the flow field. To remedy this situation, we may introduce a re-initialization of particle distribution and simultaneously transport the particle quantities in accurate way. This is called remeshing process.

We may also call the scheme as interpolation. Basically, it works on redistributing particle properties on a regular grid, then we delete the presence of the previous particle and create new set of particles that lies on the grid nodes. These new particles are carrying the interpolated fluid properties, thus creating more regular property field. We may perform the scheme after some time steps. Since we are using Vortex-In-Cell method, which requires the updated value of properties (vorticity and velocity) on the grid every time step, we perform particle re-initialization every time step.

Considering the set of particles $\{(x_p, \omega_p)\}$, the particle-mesh interpolation maps the particle property onto grid nodes with grid spacing h using the following expression:

$$\omega_{grid} = \sum_p \omega_p W\left[\frac{1}{h}(x_p - x_{grid})\right] \quad (8)$$

where W is the remeshing kernel. The equation above is applicable only for one dimensional remeshing scheme. In two and three dimensions, this operation involves a product of one-dimensional remeshing kernel. We may now introduce the third order M4' interpolation kernels we use in the solver.

$$\begin{aligned} M_4' &= 0, && if\ |x| > 2 \\ M_4' &= \frac{1}{2}(2-|x|)^2(1-|x|), && if\ 1 \le |x| \le 2 \\ M_4' &= 1 - \frac{5}{2}x^2 + \frac{3}{2}x^3, && if\ 1 \ge |x| \end{aligned} \quad (9)$$

We can see from the equation above that the $M_4$' interpolation kernels only spread a particle contribution to the grid within distance less than two grid spacing. Grid-nodes with distance greater than two spacing will receive zero contribution from the presence of the particle. We may have noted previously that we need also to do mesh to particle (M2P) interpolation. Rossinelli [13] suggests that M4' scheme will also be a good scheme to interpolate property values from the nodes to the particles. We just have to sum all contributions from grid nodes to a single particle, and the rest of the algorithm remains the same.

**Solid boundary model: The Brinkman penalization**

The no-slip condition at solid surfaces may be imposed using Brinkman penalization term by adding it to the Navier-Stokes equation. We write down penalization in terms of velocity as the following:

$$\frac{d\omega}{dt} = \nu\nabla^2\omega + \nabla \times \left[\lambda\chi(\underline{u}_s - \underline{u})\right] \quad (10)$$

where $\chi$ is the solid mask imitating Dirac delta function, and its value is 1 inside the solid and 0 in the fluid. Another parameter appears on equation 10 is $\lambda$, the penalization parameter [$s^{-1}$], which is equivalent to the inverse of porosity. The velocities, $u_s$ and $u$ describe the solid velocity and velocity field in the domain respectively.

Rasmussen [10] announced that it is desirable to choose $\lambda T >> 1$, where T is the flow characteristic time (non-dimensional). Instead solving penalization as source term (just like diffusion), Rasmussen [10] introduced a split step to perform penalization (in term of velocity) technique as the following:

VOL. 12, NO. 10, MAY 2017 ISSN 1819-6608
ARPN Journal of Engineering and Applied Sciences



| | |
|---|---|
| $\underset{\sim}{\tilde{u}}^{n+1} = \dfrac{\underline{u}^{n+1} + \lambda\Delta t\chi \underline{u}_s}{1+\lambda\Delta t\chi}$ <br> $\tilde{\omega}^{n+1} = \nabla \times \underline{\tilde{u}}^{n+1}$ | (11) |

where the tilde denotes that the result is not the final solution of the time step (since we still have to calculate the diffusion term). This technique facilitates the use of high λ values but with an increasingly discontinuous velocity field as we use step function of χ. The effect of using this scheme is we will experience the residual velocity field left in the solid interior with the order of 1/ λΔt [10]. To overcome this, we may evaluate the penalization term explicitly using similar split-step algorithm by considering λ=1/ Δt.

| | |
|---|---|
| $\underline{\tilde{u}}^{n+1} = \dfrac{\underline{u}^{n+1} + \chi \underline{u}_s}{1+\chi}$ <br> $\underline{\tilde{u}}^{n+1} = (1-\chi)\underline{u}^{n} + \chi \underline{u}_s$ | (12) |

It is convenient to introduce the penalization term as a "correction term" since replacing vorticity field by finite difference equation to calculate equation 12 will lead to significant numerical diffusion of vorticity field [10]. This formulation can be mathematically written as:

| | |
|---|---|
| $\Delta\underline{u} = \underline{\tilde{u}}^{n+1} - \underline{u}^{n} = \chi(\underline{u}_s - \underline{u}^{n})$ | (13) |
| $\Delta\omega = \nabla \times \Delta\underline{u}$ | (14) |
| $\tilde{\omega}^{n+1} = \omega^{n} \times \Delta\omega$ | (15) |

Practically, in this work, we employ the explicit scheme of penalization term because of its simplicity and its stability. Generally, the χ (the penalization function) should have the value of 1 inside the body and 0 outside the body. This will distinguish the fluid and solid region by eliminating the fluid velocity inside the solid. This will create a very high gradient in velocity, and creating a very high magnitude of vorticity in the solid obstacle. In order to overcome this problem, we introduce a mollified step function.

The detail of the mollified penalization function χ is given based on a signed distance transform φ of the obstacle [13] for a cylinder:

| | |
|---|---|
| $\chi(x) = \dfrac{1}{2} + \dfrac{1}{2}\cos[\pi\alpha(\varphi(x))]$ | (16) |
| $\varphi(x) = \lvert x - x_c \rvert - r_0$ | (17) |
| $r_0 = \dfrac{\left[D^2\pi^2 - \varepsilon^2(\pi^2-8)\right]^{1/2}}{2\pi}$ | (18) |

| | |
|---|---|
| $\alpha(r) = 0; \quad r < r_0 - \varepsilon/2$ <br> $\alpha(r) = 1; \quad r > r_0 + \varepsilon/2$ <br> $\alpha(r) = \dfrac{1}{2} + \dfrac{x - r_0}{\varepsilon}; \quad r \in [r_0 - \varepsilon/2, r_0 + \varepsilon/2]$ | (19) |

where ▯ is the mollification parameter with the value of $\varepsilon = 2\sqrt{2}h$ ,with h representing the grid spacing. We can set the value of $\varepsilon$ larger, but mostly present works on VIC use the value between $\varepsilon = 2\sqrt{2}h$ to $\varepsilon = 2\sqrt{3}h$ [10,13]. D is the diameter of the cylinder. Then we have $r_0$ to be considered as the radius where the function returns the value of 0.5. For a generally shaped body, we use the same function of χ, but with different approach to calculate distance of nearest nodes to the solid panels.

## AEROELASTIC MODEL OF TWO DIMENSIONAL SOLID BODY

The equation of motion for the two dimensional solid body depicted in Figure-1 can be generally written as:

| | |
|---|---|
| $M\ddot{X} + C\dot{X} + KX = F(t),$ | (20) |

M, C, K represent mass matrix, damping matrix, and stiffness matrix respectively. Xis the motion variable of the solid, with two modes h and θ for heaving and pitching movement. Load vector Fcontains two components, the unsteady aerodynamic force and moment.

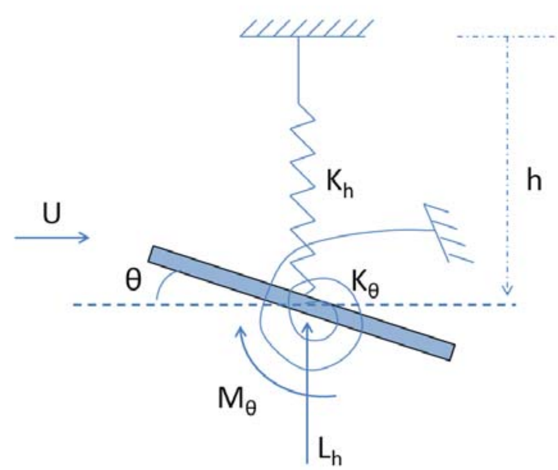


**Figure-1.** Aeroelastic model for two degree of freedom body.

Flutter derivatives is the measure which shows the contribution of translational and rotational displacement and their time-derivatives to the value of unsteady aerodynamic force and moment acted on the body. The unsteady aerodynamic force and moment can be expressed in terms of non-dimensional derivatives by the following linear relation [7]:

VOL. 12, NO. 10, MAY 2017 ISSN 1819-6608
ARPN Journal of Engineering and Applied Sciences

www.arpnjournals.com

| | |
|---|---|
| $L_h^* = KH_1^*\dot{h} + KH_2^*\dot{\theta} + K^2H_3^*\theta + K^2H_4^*h$<br>$M_\theta^* = KA_1^*\dot{h} + KA_2^*\dot{\theta} + K^2A_3^*\theta + K^2A_4^*h,$ | (21) |

where $K = B\omega/U$ and $A_1^*$, $A_2^*$, $A_3^*$, $A_4^*$, $H_1^*$, $H_2^*$, $H_3^*$, $H_4^*$ are the flutter derivatives. B is the length of the body. It is convenient to introduce the non-dimensionalized version of equation 21 as the following:

| | |
|---|---|
| $\ddot{h}^* + 2\zeta_h(\frac{2\pi}{U_h})\dot{h}^* + (\frac{2\pi}{U_h})^2 h^* = \frac{L_h^*}{n_h}$<br>$\ddot{\theta}^* + 2\zeta_\theta(\frac{2\pi}{U_\theta})\dot{\theta}^* + (\frac{2\pi}{U_\theta})^2 \theta^* = \frac{M_\theta^*}{n_\theta}.$ | (22) |

Substituting Equation 21 to the right hand side of Equation 22 we obtain:

| | |
|---|---|
| $\ddot{h}^* + 2\zeta_h K_h \dot{h}^* + (K_h)^2 h^* =$<br>$\frac{1}{n_h}(KH_1^*\dot{h} + KH_2^*\dot{\theta} + K^2H_3^*\theta + K^2H_4^*h)$<br>$\ddot{\theta}^* + 2\zeta_\theta(K_\theta)\dot{\theta}^* + (K_\theta)^2\theta^* =$<br>$\frac{1}{n_\theta}(KA_1^*\dot{h} + KA_2^*\dot{\theta} + K^2A_3^*\theta + K^2A_4^*h),$ | (23) |

where $K_h = B\omega_h/U$ and $K_\theta = B\omega_\theta/U$. $U_h$ and $U_\theta$ represents the reduced velocity, while $\omega_h$ and $\omega_\theta$ are the angular frequency of a moving body in translational mode (heaving) and rotational mode (pitching), respectively. $n_h = m/\rho B^2$ and $n_\theta = I/\rho B^4$ represents the mass and inertia ratio of the bridge cross section model. The simulation must include series of pure heaving oscillations and also pure pitching oscillations [7] with variation in angular frequency. Then, the flutter derivatives are calculated by solving the linear systems using least square technique, with the aerodynamic force and moment obtained using the VIC.

Flutter instability occurs when the heaving and pitching modes oscillate with the same frequency [7]. Then, assuming that the oscillation motion can be represented by ($h(t) = A_h e^{iKt}, \theta(t) = A_\theta e^{iKt}$) and rewriting Equation 23 into a linear system equation, we obtain:

| | |
|---|---|
| $\begin{bmatrix} a & b \\ c & d \end{bmatrix}\begin{pmatrix} A_h \\ A_\theta \end{pmatrix} = \begin{pmatrix} 0 \\ 0 \end{pmatrix}$ | (24) |
| $a = -K^2 + (2\zeta_h K_h K)i + K_h^2 -$<br>$\left[(KH_1^* i + K^2H_4^*)/n_h\right]$<br>$b = -\left[(KH_2^* i + K^2H_3^*)/n_h\right]$<br>$c = -\left[(KA_1^* i + K^2A_4^*)/n_\theta\right]$<br>$d = -K^2 + (2\zeta_\theta K_\theta K)i + K_\theta^2 -$<br>$\left[(KA_2^* i + K^2A_3^*)/n_\theta\right].$ | (25) |

In order to avoid trivial solutions, the determinant of $\begin{bmatrix} a & b \\ c & d \end{bmatrix}$ should be set to zero. $K$ can be assumed to be a complex number, $K = K_R + iK_i$. $K_i$=0 is considered as the critical condition that indicates when flutter occurs.

## CASE STUDY: FLUTTER SPEED OF FORTH ROAD BRIDGE

Prediction of the flutter speed for the Forth-Road Bridge is conducted using flutter derivatives obtained directly from VIC simulation. Forced-translation and forced-rotation simulations are performed using VIC to simulate flow over Forth-Road Bridge deck geometry as shown in Figure-2. Table-1 lists the parameters for the simulation [7, 19]. The values of angular frequency (ω) are 0.5, 1, 2, and 3 rad/s for both translational (heaving) and rotational (pitching) mode. The grid spacing used in this case is 0.025 in both x, and y direction with 0.01 s time step. In the simulation, we rescale the model so that the length will be 1 m.

Two results of flutter derivatives calculation are shown in Figure-3. $A_3$* and $H_4$* are chosen to represent the cross-flutter derivative. These derivatives are responsible to the occurence of lift generation due to rotational displacement ($A_3$*) and aerodynamic moment due to translational displacement ($H_4$*). The flutter speed can be inferred from the plot of $K_i/K_\theta$ versus reduced velocity of torsional mode ($U_\theta$), as presented in Figure-4. Flutter occurs when the value of $K_i$ (imaginary component of $K$, reduced frequency) intercepts the horizontal axis line from positive value to negative value, or simply stated when $K_i = 0$.

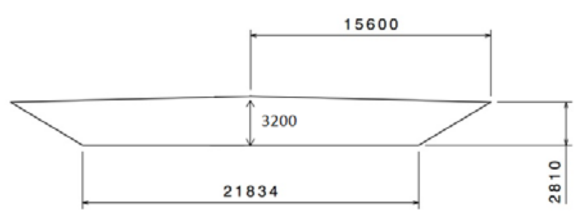


**Figure-2.** Forth-road bridge deck geometry used on the simulation (units in mm), taken from reference [7].

VOL. 12, NO. 10, MAY 2017 ISSN 1819-6608
ARPN Journal of Engineering and Applied Sciences

www.arpnjournals.com

**Table-1.** Simulation parameters.

| Reynolds Number | 10000 |
|---|---|
| Chord length (B) | 1 (m) |
| Thickness ratio (t/B) | 10 (%) |
| Airspeed (U) | 1 m/s |
| Width (chord) | 31.2 m |
| Inertia | 2.13 x $10^6$ $kgm^2$ |
| Mass | 17.3 ton/m |
| Natural frequency of heaving mode | 0.174 Hz |
| Natural frequency of pitching mode | 0.4 Hz |

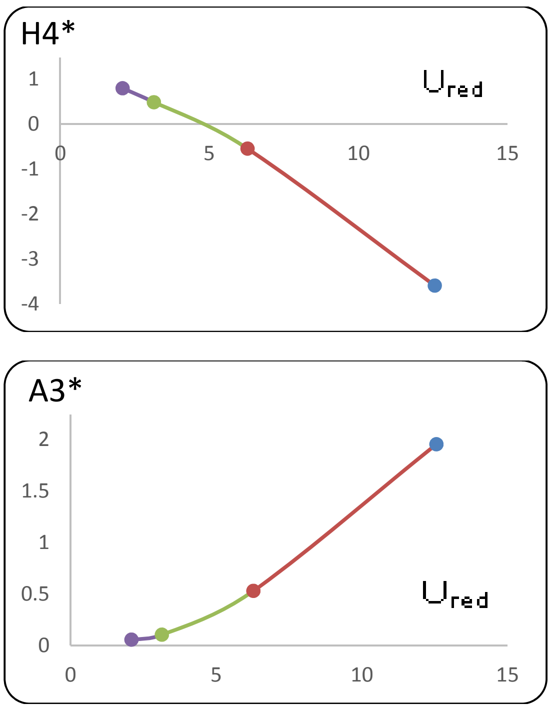


**Figure-3.** Example of flutter derivatives calculation results A3*, H4* vs $U_{red} = 2\pi/K$.

Numerical flutter analysis for the Forth Road Bridge had been published by Robertson [7] using mesh-based CFD for the actual cross-sectional geometry of the bridge and Zuhal [19] using Discrete Vortex Method using only flat plate model. The comparison between current result, reference [7], and experimental work is presented below (in terms of non-dimensional $U_\theta$):

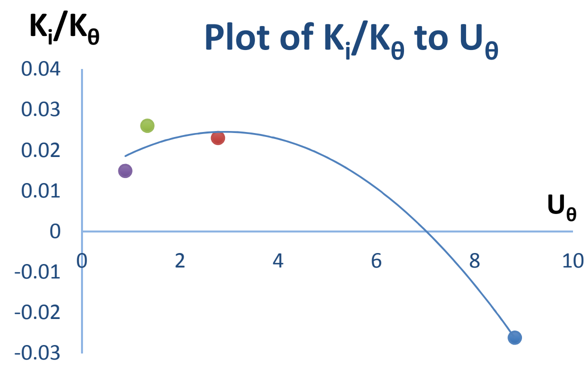


**Figure-4.** Plot of $K_i/K_\theta$ to $U_\theta$.

| | Current result | Robertson [7] (Mesh-based) | Experimental result |
|---|---|---|---|
| $U_{\theta\ critical}$ | 6.85 | 6.21 | 6.35± 0.6 |

The current work differs only about 8% to the reference (experimental result). This aberration, once again, is predicted to occur because of the computational settings, especially the grid spacing and time integration step. The present work only uses a relatively coarse grid with relatively large increment of time, thus yields to a relatively inaccurate result. However, grid refinement will lead to the escalation of the computational cost. Further parameter study is needed to optimize the balance between accuracy and cost. However, for this case, as the difference is acceptable and lies inside the experimental result range, this technique can be claimed as a good approximation to predict flutter speed of a long span bridge.

## CONCLUSIONS

In this study, we have developed a numerical method to predict flutter of a long-span bridge. The developed hybrid CFD solver, the Vortex-In-Cell (VIC), can simulate the unsteady flow around an oscillating bridge deck model in a series of forced-vibration computational experiment. It is found that the flutter speed obtained using VIC simulations is in good agreement with reference values found in literature and also the experimental results. Therefore, the developed numerical method could be utilized to complement the more expensive experimental methods in long-span bridge flutter prediction analysis.

## ACKNOWLEDGEMENT

This research is funded by ITB Research and Innovation Program 2015.

## REFERENCES

[1] Cottet G. H. and Koumoutsakos P. D. 2009. Vortex method, theory and practice. Cambridge University Press, United Kingdom.

[2] Dung D. V. and Zuhal L.2011. Two dimensional fast lagrangian vortex method for fluid structure interaction analysis. Aeroelastic Problem, Regional Conference on Mechanical and Aerospace Technology.

[3] Huang M. J., Su H. X. and Chen L. C. 2009. A fast resurrected core-spreading vortex method with no-slip boundary conditions. Journal of Computational Physics. 228(6): 1916-1931.

[4] Morgenthal G. 2002. Aerodynamic analysis of structures using high-resolution vortex particle methods (Doctoral dissertation, University of Cambridge).

[5] Nagao F., Utsunomiya H. and Murata S. 1997. Improvement of pitching moment estimation of an oscillating body by discrete vortex method. Journal of wind engineering and industrial aerodynamics. 67: 337-347.

[6] Ploumhans P. and Winckelmans G. S. 2000. Vortex methods for high-resolution simulations of viscous flow past bluff bodies of general geometry. Journal of Computational Physics. 165(2): 354-406.

[7] Robertson I., Sherwin S. J. and Bearman P. W. 2003. Flutter instability prediction techniques for bridge deck sections. International Journal for Numerical Methods in Fluids 43(10-11): 1239-1256.

[8] Lan L., Feng J. I., Jian-ren F. A. N. and Ke-fa C. E. N. 2005. Recent development of vortex method in incompressible viscous bluff body flows. Journal of Zhejiang University Science A. 6(4): 283-288.

[9] Cottet G. H., Gallizio F., Magni, A. and Mortazavi I. 2010. A vortex immersed boundary method for bluff body flows. Proceedings of Symposium on Development and Applications of Immersed Boundary Methods. Montreal, Canada. Pp. 2409-2414.

[10] Rasmussen J. T. 2008.Master thesis: a penalization interface method for 3d particle vortex methods. Technical University of Denmark.

[11] Rasmussen J. T. 2011. Particle methods in bluff body aerodynamics. Technical University of Denmark.

[12] Sepnov Alex J. 2009.Master thesis: development of three-dimensional vortex element method for high resolution flow simulation. Institut Teknologi Bandung,

[13] Rossinelli D. 2011. Multiresolution flow simulations on multi/many-core architectures (Doctoral dissertation, ETH).

[14] Hoffmann K. A. 2000. Computational Fluid Dynamics Volume I. Austin: Engineering Education System.

[15] Barba L. A. 2004. Vortex Method for computing high-Reynolds number flows: Increased accuracy with a fully mesh-less formulation (Doctoral dissertation, California Institute of Technology).

[16] Angot P., Bruneau C. H. and Fabrie P. 1999. A penalization method to take into account obstacles in incompressible viscous flows. Numerische Mathematik. 81(4): 497-520.

[17] Peskin C. S. 2002. The immersed boundary method. Acta numerica. 11: 479-517.

[18] Coquerelle M. and Cottet G. H. 2008. A vortex level set method for the two-way coupling of an incompressible fluid with colliding rigid bodies. Journal of Computational Physics. 227(21): 9121-9137.

[19] Zuhal L. R., Febrianto E. V. and Dung D. V. 2014. Flutter speed determination of two degree of freedom model using discrete vortex method. Applied Mechanics and Materials. 660: 639-643.